International Journal of Women's Health

Dovepress
Taylor & Francis Group

Open Access Full Text Article

ORIGINAL RESEARCH

Identification of Key Mitochondrial Autophagy-Related Genes in Fetal Growth Restriction

Yanru Yao, Gang Lei, Guangxin Pan, Guoping Xiong, Jian Shen

Obstetric, Centre Hospital of Wuhan, Huazhong University of Science and Technology, Wuhan, Hubei, 430014, People's Republic of China

Correspondence: Guoping Xiong; Jian Shen, Obstetric, Centre Hospital of Wuhan, Huazhong University of Science and Technology, No. 26, Shengli Street, Jiang'an District, Wuhan, Hubei, 430014, People's Republic of China, Email Hyh0120@163.com; sjck1983@126.com

Objective: To identify key mitochondrial autophagy-related genes (MARGs) in fetal growth restriction (FGR)and evaluate their diagnostic potential through bioinformatics and machine learning approaches.

Methods: The GSE24192 dataset were obtained from Gene Expression Omnibus data base (GEO). Differentially expressed genes (DEGs) were identified using differentially expressed analysis. Mitochondrial autophagy-related genes (MARGs) were identified using GeneCards. Gene Ontology (GO) and Kyoto Encyclopedia of Genes and Genomes (KEGG) enrichment analyses were performed with the clusterProfiler package. Protein-protein interaction (PPI) network was constructed using STRING, and key genes were selected using machine learning. Receiver operating characteristic (ROC) curves assessed diagnostic performance of key genes. Immune infiltration analysis was used to evaluated immune microenvironment. The miRNAs were predicted in TargetScan website.

Results: A total of 42 MARGs were identified in FGR samples, and three key genes (THBS1, RAB15, LMO7) were selected through machine learning methods. These genes showed high diagnostic potential with area under the curve (AUC) values of 0.97, 0.95, and 0.92, respectively. Immune infiltration analysis revealed significant increase of CD8+ T cells, endothelial cells, and macrophages in FGR samples. Correlation analysis indicated THBS1 was positively related to several immune cells, while RAB15 and LMO7 were negatively related to several immune cells. The miRNA-mRNA regulatory network revealed four miRNAs potentially regulating these key genes.

Conclusion: In conclusion, our study identified THBS1, RAB15, and LMO7 as key mitochondrial autophagy-related genes in FGR, with potential as diagnostic biomarkers.

Keywords: fetal growth restriction, mitochondrial autophagy, immune, machine learning, nomogram

Introduction

Fetal growth restriction (FGR) is a severe complication during pregnancy, affecting 5–10% of pregnancies globally, and it is a significant cause of perinatal morbidity and mortality.[1] FGR is primarily caused by placental insufficiency, where the placenta fails to meet the oxygen and nutritional needs of the growing fetus.[2] It usually leads to preterm birth, low birth weight, and long-term health impacts for the child, such as neurodevelopmental delays and cardiovascular diseases.[3,4] Despite extensive research, the underlying molecular mechanisms leading to FGR are still not fully understood. Traditional diagnostic methods, such as Doppler ultrasound, typically detect FGR at a late stage, limiting effective interventions.[5] Therefore, identifying specific molecular biomarkers and understanding the pathways involved in FGR development are critical for early diagnosis and targeted treatments.

Mitochondrial autophagy is a key cellular process responsible for the degradation and recycling of damaged mitochondria.[6] It plays a vital role in maintaining cellular homeostasis, particularly in tissues with high energy demands.[7,8] Abnormal mitochondrial autophagy is associated with various diseases, including neurodegenerative disorders, cardiovascular diseases, and cancer.[9] In such cases, dysregulated mitochondrial autophagy often leads to impaired cellular metabolism and increased oxidative stress, thereby promoting disease progression.[10,11] Recent studies suggest

Received: 7 December 2024
Accepted: 24 April 2025
Published: 5 May 2025

that mitochondrial autophagy may also play a role in placental disorders, including preeclampsia and FGR.[12,13] The placenta, being a metabolically active organ, heavily relies on mitochondrial function to support fetal growth.[14] Dysregulated mitochondrial autophagy in the placenta can impair mitochondrial quality control, leading to placental dysfunction and subsequent FGR.[14–16] At present, except some biomarkers related to inflammation in FGR had been identified,[17,18] several studies indicate that genes involved in mitochondrial autophagy can serve as diagnostic and prognostic biomarkers for other diseases, such as female lung adenocarcinoma and ovarian cancer,[19,20] suggesting that mitochondrial autophagy-related genes (MARGs) may also have diagnostic value in FGR. Machine learning algorithms, such as random forest and Lasso regression, have been widely applied in genomics to identify key biomarkers by reducing data dimensionality and improving predictive accuracy. Numerous studies have already used these methods to identify important marker genes and apply them in clinical practice.[21,22]

Given the potential link between mitochondrial autophagy and FGR, this study aimed to identify key MARGs associated with FGR using bioinformatics analysis and machine learning algorithms. By integrating gene expression data of FGR and normal placental samples, we performed differential expression analysis, pathway enrichment, and machine learning-based gene selection to uncover critical genes involved in FGR. Additionally, we explored the immune microenvironment in FGR placentas and examined the role of key genes in immune regulation. This study aims to provide new insights into the molecular mechanisms of FGR and identify potential biomarkers for early diagnosis and therapeutic intervention.

Methods

Data Acquisition and Preprocessing

The GSE24129 dataset was downloaded from the Gene Expression Omnibus data base (GEO) database. This dataset comprises placental tissue samples from 8 FGR cases and 8 healthy controls. Informed consent was obtained from each patient and the study protocol was approved by the Ethical Review Board for Human Genome Studies at Fujita Health University in these GEO dataset.[23] The data were log2-transformed and normalized prior to analysis to eliminate differences between samples and ensure data consistency. In addition, MARGs were screened using "mitochondrial autophagy" as the keyword on the GeneCard website.

Differentially Expressed Gene (DEG) Screening

The "limma" R package was used to screen the DEGs in the preprocessed data. The screening criteria were set as: adjusted p-value (FDR) less than 0.05, and |log2FoldChange(FC)| greater than 1, to filter out significantly differentially expressed genes.

Gene Ontology (GO) and Kyoto Encyclopedia of Genes and Genomes (KEGG) Enrichment Analysis

GO and KEGG enrichment analyses were performed using the clusterProfiler R package. For GO enrichment analysis, the function enrichGO() was used to identify significant entries for DEGs in biological processes (BP), molecular functions (MF), and cellular components (CC). For KEGG pathway analysis, the function enrichKEGG() was used to identify significantly enriched signaling pathways. The results were visualized using the ggplot2 R package.

Protein-Protein Interaction (PPI) Network Construction

The STRING database was used to construct a PPI network for the screened mitochondrial autophagy-related DEGs, assessing their interactions. In this network, nodes represent proteins, and edges represent interactions. The PPI network was visualized using Cytoscape software.

Machine Learning

To further filter the key genes related to FGR among the intersecting genes, three machine learning methods were applied: Random Forest (RF), Support Vector Machine (SVM), and Lasso regression. Gene expression data were subjected to feature selection and classification using these methods.

The RF algorithm was used to rank the importance of genes through "randomForest" package. The importance scores were derived from the voting results of multiple decision trees. The model error was evaluated through 5-fold cross-validation, and the top-ranked important genes were identified.

The SVM model was evaluated through 5-fold cross-validation, and the number of features was incrementally increased to determine the best performance at different feature counts. The optimal number of features was determined by the cross-validation error and accuracy curve based on "e1071" package.

Lasso regression with regularization was used to select key genes "glmnet" package. Genes corresponding to non-zero coefficients were selected based on the optimal penalty parameter (lambda).

Receiver Operating Characteristic (ROC) Curve

To assess the diagnostic performance of key genes as biomarkers, the "pROC" package was used to plot ROC curves and calculate the area under the curve (AUC) for each gene. AUC values were used to evaluate the ability of the genes to distinguish between normal and FGR samples. AUC values range from 0.5 to 1.0, with values closer to 1 indicating higher diagnostic performance. The final results were visualized using the ggplot2 package.

Risk Prediction Model Based on Key Genes and Validation

A nomogram was constructed using the "rms" R package, based on either a Cox regression model or logistic regression model. The nomogram() function was used to generate an individualized prediction model, with the calibration curve plotted using the calibrate() function. The model's predictive performance was evaluated using 1000 bootstrap iterations to assess the agreement between the model's predictions and actual outcomes. Decision curve analysis (DCA) was

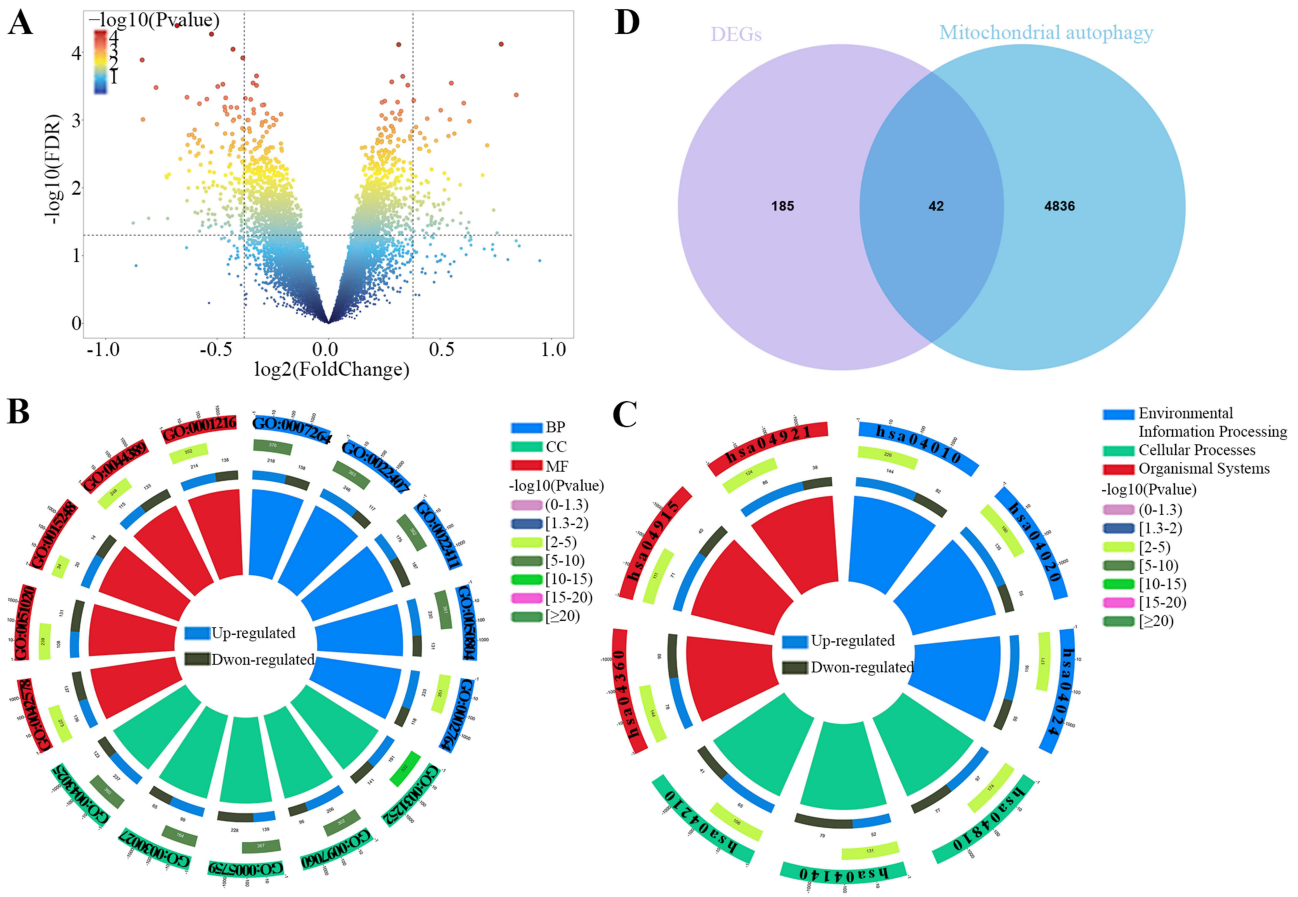

Figure 1 Differential expression and enrichment analysis of mitochondrial autophagy-related genes in FGR samples. (**A**) Volcano plot of DEGs in FGR samples. (**B**) GO enrichment analysis of DEGs. (**C**) KEGG pathway enrichment analysis of DEGs. (**D**) Venn diagram showing the intersection of DEGs and MARGs.

https://doi.org/10.2147/IJWH.S510947

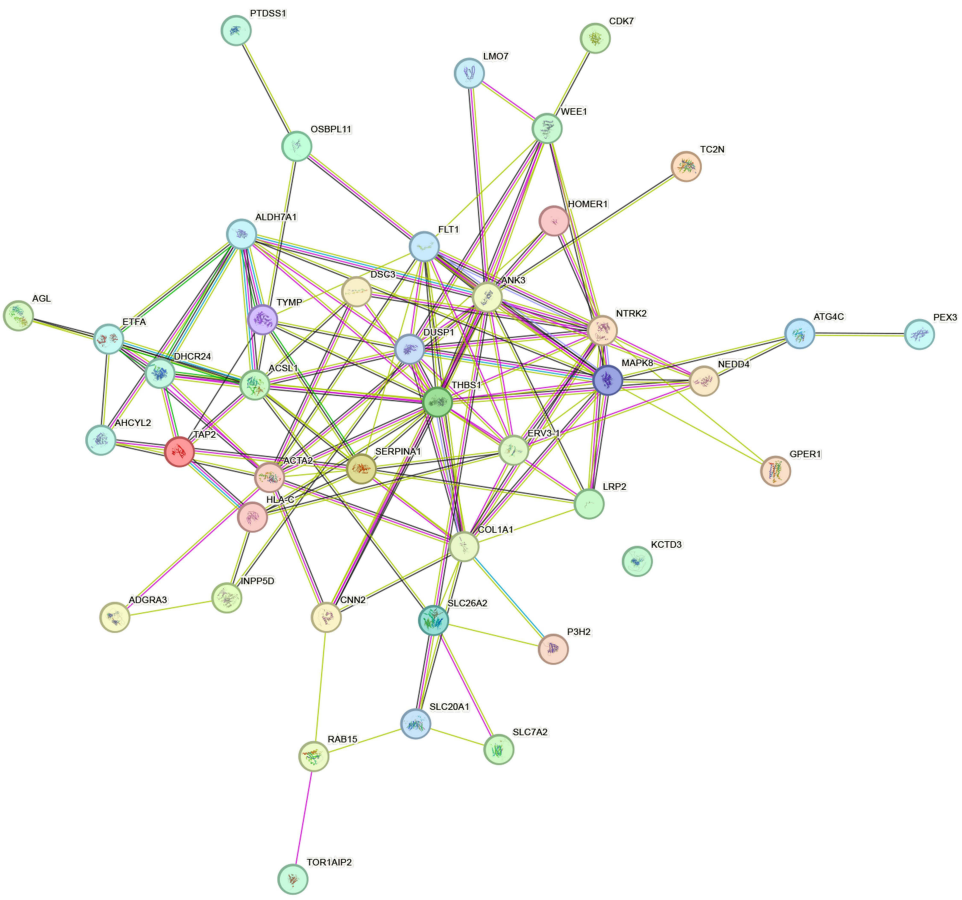

Figure 2 PPI network of intersecting genes.

performed using the "stdca" R package's dca() function to assess the clinical net benefit of the model at different threshold probabilities.

Immune Infiltration Analysis

Immune cell infiltration was analyzed using the "IOBR" R package, applying two commonly used algorithms (EPIC and xCell), to assess immune cell composition and the tumor microenvironment in the samples.

EPIC algorithm: EPIC was used to estimate the relative abundance of different types of immune cells in the tumor samples, particularly T cells, B cells, macrophages, and others. EPIC analysis was performed using the epic() function, which outputs the proportions of each cell type.

xCell algorithm: The xCell algorithm was used to comprehensively analyze the relative abundance of 34 types of immune and stromal cells. The xcell() function was employed for this analysis, and the results provided enrichment scores for both immune and stromal cells.

miRNA Target Gene Prediction and Regulatory Network Construction

To further investigate the regulatory mechanisms of key genes, we used the TargetScan database to predict potential miRNAs targeting key genes. The collection of miRNAs targeting these key genes was filtered, and an intersection analysis was performed to identify commonly regulated miRNAs. The STRING database was then used to construct a PPI network for the key genes, identifying their interaction relationships. Combining the results of the PPI network and miRNA target prediction, a miRNA-mRNA regulatory network was constructed using Cytoscape software to visualize the regulatory relationships between key genes and miRNAs.

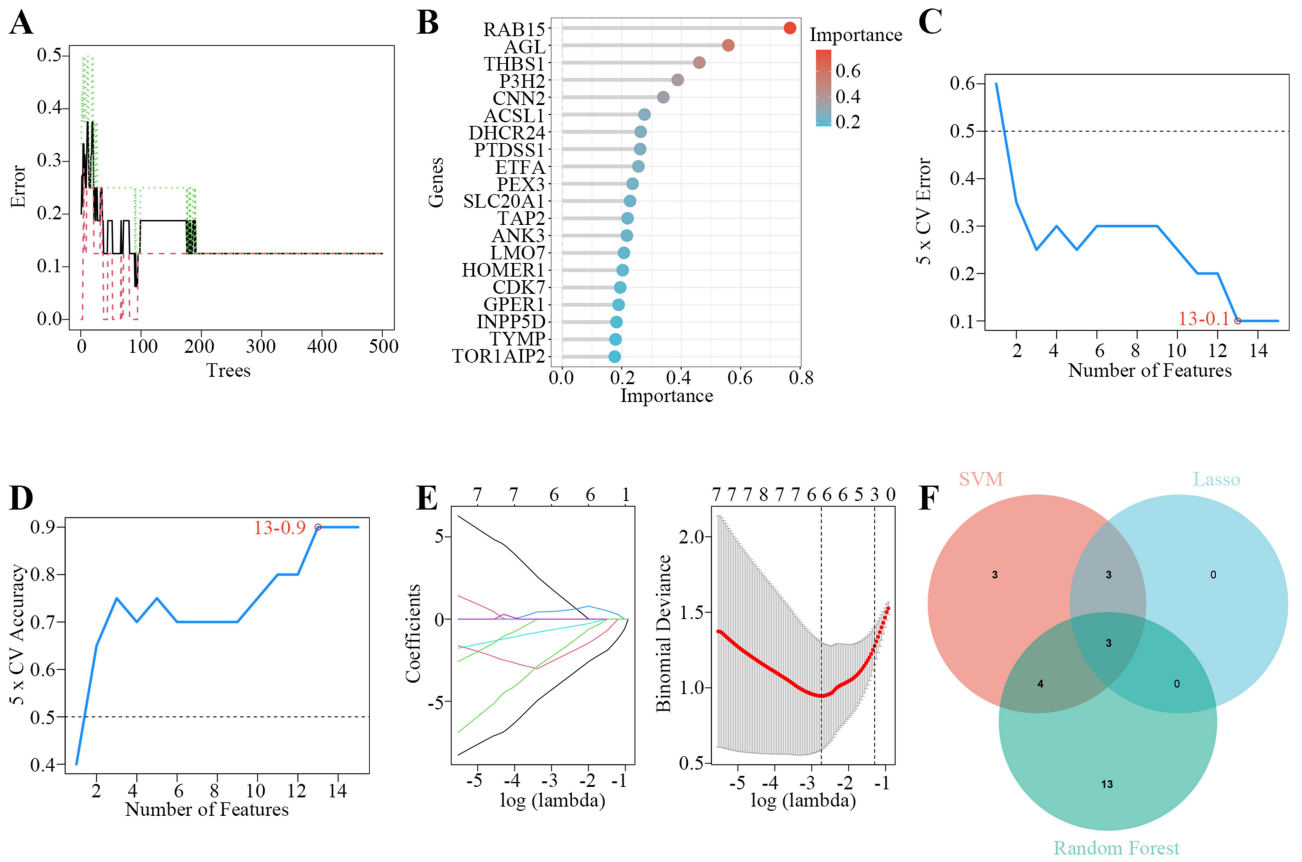

Figure 3 Feature selection of intersecting genes using RF, SVM, and Lasso regression methods. (**A**) Error variation curve in the RF model. (**B**) Importance ranking of genes in the RF model. (**C**) Cross-validation error in the SVM model with varying feature counts. (**D**) Cross-validation accuracy in the SVM model with varying feature counts. (**E**) Coefficient path in Lasso regression. (**F**) Venn diagram showing the intersecting genes selected by SVM, RF, and Lasso regression methods.

Statistical Analysis

All statistical analyses were performed using R software (version 4.4.1) and SPSS. The diagnostic value of hub mitochondrial autophagy-related genes (MDRGs) was evaluated with receiver operating characteristic (ROC) curves. A paired *t*-test was used for two-group comparisons. The correlation between two groups were analyzed using Spearman correlation analysis. All tests were two-sided, and a p-value of less than 0.05 was regarded as indicating statistical significance across all tests.

Results

The Selection of DEGs and Enrichment Analysis

In this study, we utilized the GSE24192 dataset from the GEO database to analyze the differences in gene expression between fetal growth restriction (FGR) samples and normal placental samples. By applying a filtering criterion of log2FoldChange ≥ 1 and q-value ≤ 0.05, a volcano plot was generated (Figure 1A), identifying a large number of significantly differentially expressed genes (DEGs), with 79 genes being significantly upregulated and 148 significantly downregulated.

Further GO and KEGG enrichment analyses were conducted on these overlap genes. As shown in Figure 1B, in the aspect of BP, DEGs were mainly involved in small GTPase mediated signal transduction, regulation of cell-cell adhesion and immune response-regulating signaling pathway. Besides, in the term of MF, DEGs play essential roles in DNA-binding transcription activator activity, phosphoric ester hydrolase activity and ubiquitin-like protein ligase binding (Figure 1B). In addition, these DEGs were mainly existed in cell leading edge, mitochondrial matrix and neuronal cell body (Figure 1B). KEGG pathway enrichment analysis showed that the intersecting genes were significantly enriched in autophagy, apoptosis and MAPK signaling pathway (Figure 1C).

https://doi.org/10.2147/IJWH.S510947

Subsequently, an intersection analysis was performed between these DEGs and MARGs identified from the GeneCard database, resulting in 42 overlap genes (Figure 1D).

The Construction of PPI Network

Using the STRING database, we constructed a PPI network for the 42 mitochondrial autophagy-related DEGs (Figure 2). The PPI network illustrated the interactions between proteins encoded by these genes. The nodes represent proteins, and the edges represent interactions. Different colors of the edges indicate different types of interaction sources, including experimental validation, database analysis, and text mining.

Machine Learning Model for Key Gene Selection

Three machine learning methods—RF, SVM, and Lasso regression—were used to perform feature selection on the intersecting genes, with the results shown in Figure 3. Figure 3A shows the error variation in the RF model, with the error gradually decreasing and stabilizing as the number of decision trees increases. Figure 3B presents the importance ranking of genes in the RF model, where RAB15, AGL, and THBS1 were highly ranked. Figure 3C and D illustrate the cross-validation error and accuracy variation in the SVM model at different feature counts, with the best model achieved at 13 features, where the error was lowest and accuracy highest. Figure 3E displays the coefficient path of Lasso regression, where the optimal number of features was determined at log(lambda) = −2.3, selecting six key features. The results of the three machine learning methods were presented in a Venn diagram (Figure 3F), which identified three intersecting genes that may play critical roles in the regulation of FGR.

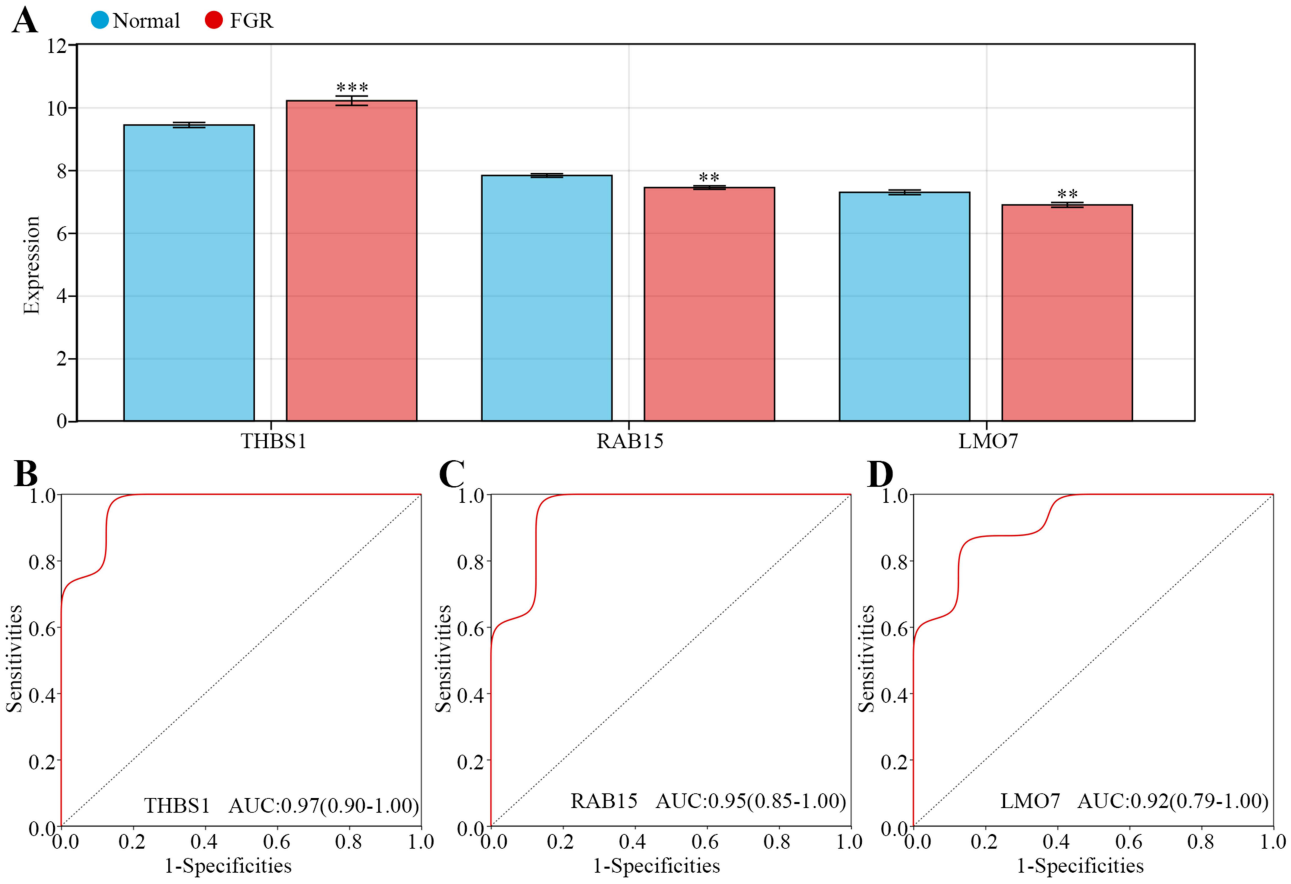

Figure 4 Expression and diagnostic performance analysis of three key genes in normal and FGR samples. (**A**) Bar plots showing the expression differences of THBS1, RAB15, and LMO7 between normal and FGR samples. (**B**) ROC curve and AUC value for THBS1. (**C**) ROC curve and AUC value for RAB15. (**D**) ROC curve and AUC value for LMO7.

The Expression and Diagnostic Value of Key Genes

To further validate the potential role of the intersecting genes in FGR, we performed expression analysis and evaluated the diagnostic efficacy of three key genes: THBS1, RAB15, and LMO7. Figure 4A shows the expression differences of these three genes between normal and FGR samples. The results indicate that THBS1 was significantly upregulated in FGR samples, while RAB15 and LMO7 were significantly downregulated in the FGR group. ROC analysis showed that the AUC values were 0.97 (95% CI: 0.90–1.00) for THBS1, 0.95 (95% CI: 0.85–1.00) for RAB15, and 0.92 (95% CI: 0.79–1.00) for LMO7 (Figure 4B–D), indicating that these genes have high diagnostic potential in distinguishing FGR from normal samples.

Construction and Clinical Evaluation of the Nomogram

Subsequently, to further enhance the clinical significance of the key genes in diagnosis, we constructed a nomogram based on the expression profiles of the three genes (Figure 5A). The expression levels of each gene were converted into corresponding scores through the nomogram, with the total score used to calculate the probability of FGR risk. A higher total score corresponded to a higher risk of FGR. The calibration curve of the nomogram closely aligned with the ideal 45-degree diagonal line, indicating good calibration performance (Figure 5B). Additionally, decision curve analysis (DCA) results showed that the model yielded higher net benefits across a wide range of threshold probabilities (0.1–0.8), demonstrating the model's potential clinical utility (Figure 5C).

Immune Infiltration Analysis

Since enrichment analysis indicated that DEGs were enriched in immune response-related pathways, immune infiltration analysis was conducted. EPIC results showed that the proportion of CD8+ T cells significantly decreased in the FGR group, while the proportions of endothelial cells and macrophages significantly increased (Figure 6A). xCell analysis revealed that the

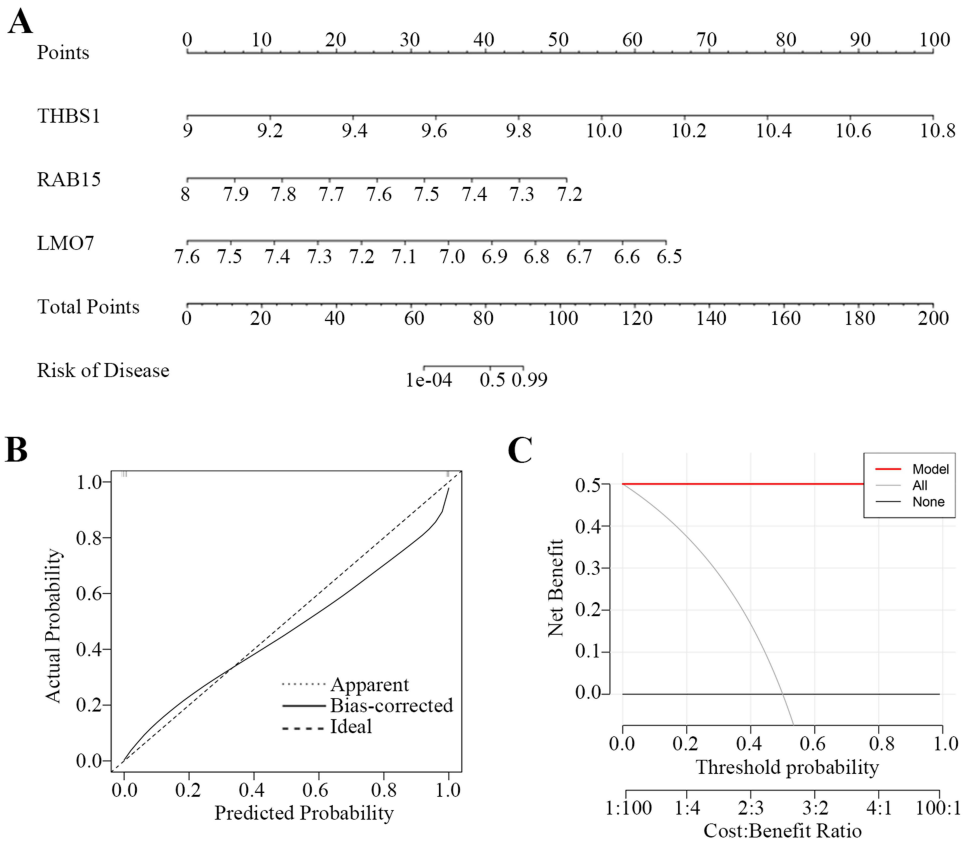

Figure 5 FGR risk prediction model and performance validation based on THBS1, RAB15, and LMO7. (**A**) Nomogram based on the three key genes. (**B**) Calibration curve of the nomogram. (**C**) DCA results for nomogram.

https://doi.org/10.2147/IJWH.S510947

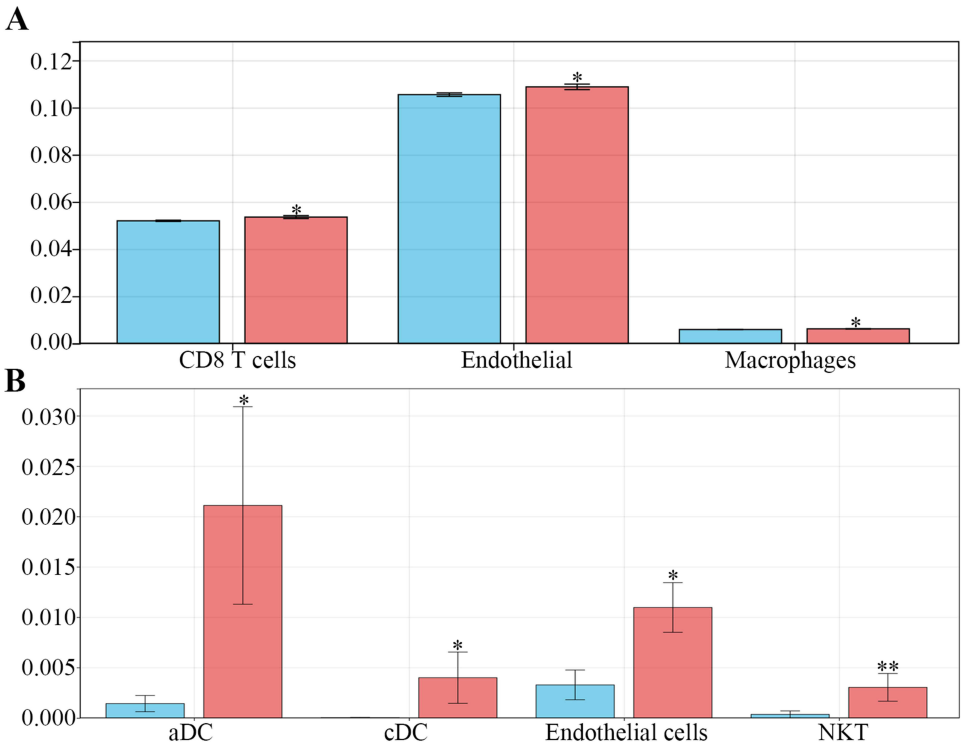

Figure 6 Immune infiltration analysis results. (**A**) Comparison of immune cell proportions estimated by the EPIC algorithm between normal and FGR samples. (**B**) Comparison of immune cell proportions estimated by the xCell algorithm between normal and FGR samples. Blue represents normal samples, and red represents FGR samples. *, $p<0.05$; **$p<0.001$.

proportions of activated dendritic cells (aDCs) and endothelial cells significantly increased in FGR samples, while the proportions of classical dendritic cells (cDCs) and natural killer T (NKT) cells significantly decreased (Figure 6B).

Correlation Analysis Between Key Genes and Immune Cells

To further explore the potential mechanisms underlying FGR development, we analyzed the correlations between the key genes and immune cell infiltration. Figure 7A shows that THBS1 was significantly positively correlated with aDCs, cDCs, endothelial cells, NKT cells, and CD8+ T cells. Figure 7B shows that RAB15 was significantly positively correlated with aDCs and macrophages, and showed a near-significant trend with cDCs. Figure 7C shows the correlation between LMO7 and immune cell infiltration. LMO7 was significantly negatively correlated with endothelial cells, CD8+ T cells, NKT cells, and aDCs, with the strongest correlations seen with NKT cells and endothelial cells.

The Prediction of Targeted miRNA and Construction of Regulatory Network

Finally, we constructed a regulatory network to further elucidate the interaction mechanisms between these key genes, providing a new perspective for understanding the molecular mechanisms of FGR. Figure 8A shows the intersection of miRNAs targeting THBS1, RAB15, and LMO7, predicted using TargetScan. The results suggest that four miRNAs commonly target these three genes, indicating that these miRNAs may play an important role in FGR regulation. Figure 8B shows the PPI network of THBS1, RAB15, and LMO7 constructed using the STRING database. The results indicate significant interactions between these key genes and their interacting proteins, such as ACTN4, MICAL1, and TPM4. Finally, we constructed the miRNA-mRNA regulatory network (Figure 8C) based on the PPI network and miRNA target prediction results, illustrating the regulatory relationships between miRNAs, key genes, and their interacting proteins.

Discussion

FGR is a severe obstetric complication characterized by suboptimal fetal development due to placental insufficiency. Understanding the molecular mechanisms underlying FGR is crucial for improving early diagnosis and treatment. In this

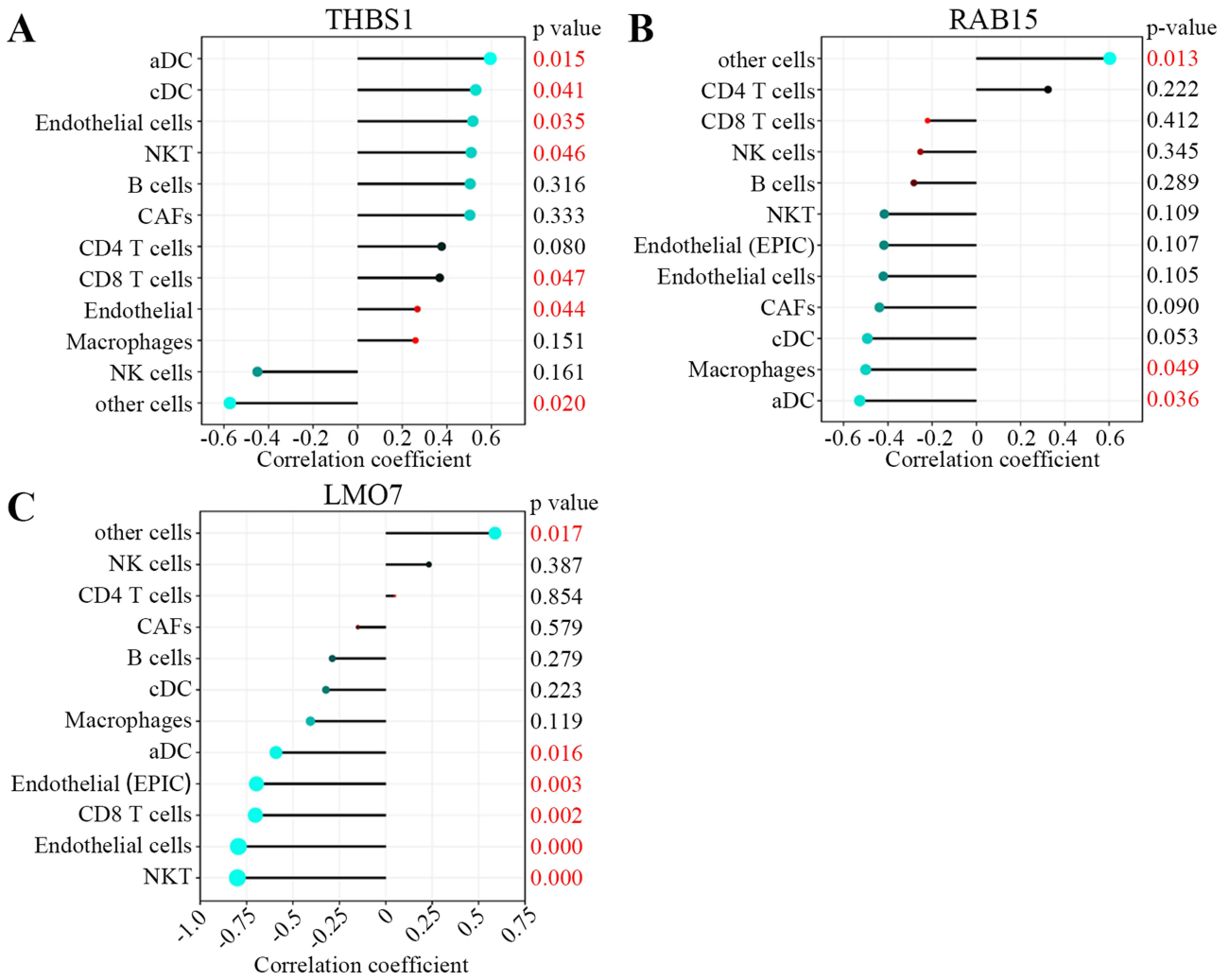

Figure 7 Correlation analysis between key genes and immune cell infiltration. (**A**) Correlation between THBS1 and immune cell infiltration. (**B**) Correlation between RAB15 and immune cell infiltration. (**C**) Correlation between LMO7 and immune cell infiltration.

study, we used differential expression analysis, GO and KEGG enrichment, and machine learning techniques to explore key molecular players involved in FGR. From the GEO dataset GSE24192, we identified DEGs between FGR and normal samples. GO and KEGG enrichment analyses revealed important pathways related to mitochondrial autophagy, cellular stress, and immune responses, all of which are known to play roles in placental development. By combining these DEGs with a set of 4878 MARGs, we identified 42 overlapping genes. Further filtering using machine learning techniques, including RF, SVM, and Lasso regression, allowed us to pinpoint three key genes: THBS1, RAB15, and LMO7. Additionally, previous studies have found elevated levels of immune cell infiltration in FGR.[24] Similarly, our immune infiltration analysis also revealed significant increases in various immune cells in the FGR group.

THBS1 is a matricellular glycoprotein involved in various physiological processes, including tissue remodeling, angiogenesis, and immune regulation.[25,26] In our study, THBS1 was significantly upregulated in FGR samples and showed high diagnostic efficacy, suggesting its potential as a biomarker for FGR. Previous literature indicates that elevated THBS1 expression can promote endothelial cell proliferation and migration, contributing to disease progression.[27] Moreover, endothelial cells may release large amounts of inflammatory factors, exacerbating inflammation and worsening the condition.[28] On the other hand, numerous studies have found that abnormal angiogenesis and reduced uterine blood flow can lead to pregnancy-related disorders such as FGR and preeclampsia.[29] THBS1 can also inhibit angiogenesis to a certain extent.[30] Our study similarly found that THBS1 was highly expressed in FGR; however, THBS1

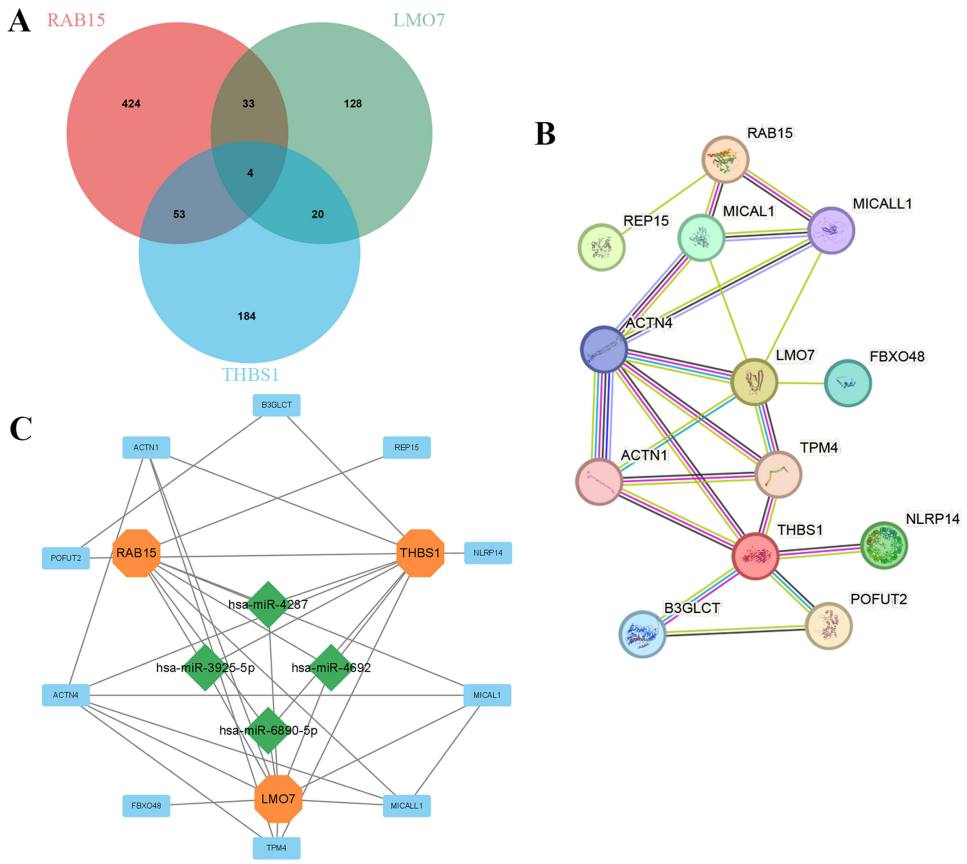

Figure 8 miRNA target prediction and regulatory network construction. (**A**) Intersection analysis of miRNAs targeting THBS1, RAB15, and LMO7. (**B**) PPI network based on STRING database showing interactions between THBS1, RAB15, LMO7, and their interacting proteins. (**C**) miRNA-mRNA regulatory network showing the regulatory relationships between miRNAs, key genes, and their interacting proteins.

did not show a strong correlation with endothelial cell infiltration. These results suggest that THBS1 may primarily contribute to FGR development by inhibiting angiogenesis, rather than by promoting endothelial cell infiltration to secrete inflammatory factors.

RAB15, a member of the RAB GTPase family, is involved in vesicle transport and the regulation of autophagy.[31] Research on RAB15 is limited. Early studies mainly focused on its role in endocytosis.[32–34] Later, researchers found that RAB15 is also involved in non-small cell lung cancer proliferation and neuroblastoma differentiation.[35,36] More recently, RAB15 was discovered to enhance the antiviral capacity of T cells by promoting DC activity,[37] suggesting that RAB15 may play a role in other immune responses as well. Our results indicate that RAB15 is negatively correlated with macrophage and DC infiltration, implying that RAB15 may regulate immune responses by inhibiting the infiltration of these cells, thereby affecting FGR development.

LMO7 is an actin-binding protein expressed in multiple tissues.[38] In cancer studies, LMO7 is upregulated in most tumor tissues, promoting cancer progression by enhancing cell proliferation and epithelial-mesenchymal transition (EMT).[39–42] However, our results indicate that LMO7 expression was significantly reduced in FGR, suggesting that LMO7 may function differently in FGR than it does in cancer. A recent study found that LMO7 can inhibit inflammation by suppressing macrophage activation.[43] Previous studies also showed that an increase in the M1 macrophage phenotype leads to a rise in total macrophages in pregnancy-related disorders such as preeclampsia.[44–46] Our immune infiltration analysis also revealed a significant increase in macrophage infiltration. However, the correlation between macrophages and LMO7 was not significant, possibly because our analysis included both pro-inflammatory M1 macrophages and anti-inflammatory M2 macrophages.

In summary, this study successfully identified three key MARGs (THBS1, RAB15, and LMO7) that show strong diagnostic potential. Moreover, these genes may influence energy metabolism by regulating mitochondrial autophagy, immune responses, and angiogenesis, thereby inhibiting placental energy supply to the fetus and leading to FGR. Future studies should validate these biomarkers in larger cohorts and explore their therapeutic significance. However, several limitations should be considered. First, the dataset used for analysis was relatively small, and further validation in larger, independent cohorts is needed to confirm the diagnostic and mechanistic findings. Additionally, while bioinformatics predictions provide valuable insights, in vitro and in vivo functional studies are required to validate the roles of these key genes.

Overall, this study offers new insights into the molecular mechanisms of FGR, particularly the involvement of mitochondrial autophagy and immune responses. Future research should explore the functions of these key genes in FGR and assess their potential as diagnostic and therapeutic targets.

Data Sharing Statement

The datasets generated during and/or analyzed during the current study are available from the corresponding author on reasonable request.

Ethics Approval

The Ethics Committee of Centre Hospital of Wuhan, Huazhong University of Science and Technology deemed that this research is based on open-source data, so the need for ethics approval was waived.

Author Contributions

All authors made a significant contribution to the work reported, whether that is in the conception, study design, execution, acquisition of data, analysis and interpretation, or in all these areas; took part in drafting, revising or critically reviewing the article; gave final approval of the version to be published; have agreed on the journal to which the article has been submitted; and agree to be accountable for all aspects of the work.

Funding

This work was supported by the Natural Science Foundation of Hubei Province (2021CFB526), the Scientific Research Project of the Hubei Provincial Health Committee (WJ2021F003) and the Wuhan Municipal Health Commission (WX21D01).

Disclosure

The authors report no conflicts of interest in this work.

References

1. Broere-Brown ZA, Schalekamp-Timmermans S, Jaddoe VWV, Steegers EAP. Deceleration of fetal growth rate as alternative predictor for childhood outcomes: a birth cohort study. *BMC Pregnancy Childbirth*. 2019;19(1):216. doi:10.1186/s12884-019-2358-8
2. Terstappen F, Calis JJA, Paauw ND, et al. Developmental programming in human umbilical cord vein endothelial cells following fetal growth restriction. *Clin Clin Epigenet*. 2020;12(1):185. doi:10.1186/s13148-020-00980-9
3. Lawn JE, Ohuma EO, Bradley E, et al. Small babies, big risks: global estimates of prevalence and mortality for vulnerable newborns to accelerate change and improve counting. *Lancet*. 2023;401(10389):1707–1719. doi:10.1016/S0140-6736(23)00522-6
4. Hambidge KM, Westcott JE, Garces A, et al. A multicountry randomized controlled trial of comprehensive maternal nutrition supplementation initiated before conception: the women first trial. *Am J Clin Nutr*. 2019;109(2):457–469. doi:10.1093/ajcn/nqy228
5. Nardozza LM, Caetano AC, Zamarian AC, et al. Fetal growth restriction: current knowledge. *Arch Gynecol Obstet*. 2017;295(5):1061–1077. doi:10.1007/s00404-017-4341-9
6. Xu H, Yu W, Sun S, Li C, Zhang Y, Ren J. Luteolin attenuates doxorubicin-induced cardiotoxicity through promoting mitochondrial autophagy. *Front Physiol*. 2020;11:113. doi:10.3389/fphys.2020.00113
7. Gabande-Rodriguez E, Gomez de Las Heras MM, Mittelbrunn M. Control of inflammation by calorie restriction mimetics: on the crossroad of autophagy and mitochondria. *Cells*. 2019;9(1). doi:10.3390/cells9010082
8. Mohanty A, Tiwari-Pandey R, Pandey NR. Mitochondria: the indispensable players in innate immunity and guardians of the inflammatory response. *J Cell Commun Signal*. 2019;13(3):303–318. doi:10.1007/s12079-019-00507-9
9. Park SW, Jeon P, Yamasaki A, et al. Development of new tools to study membrane-anchored mammalian Atg8 proteins. *Autophagy*. 2023;19(5):1424–1443. doi:10.1080/15548627.2022.2132040

10. Chung C, Seo W, Silwal P, Jo EK. Crosstalks between inflammasome and autophagy in cancer. *J Hematol Oncol*. 2020;13(1):100. doi:10.1186/s13045-020-00936-9
11. Hamdan N, Lee CH, Wong SL, Fauzi C, Zamri NMA, Lee TH. Prevention of enzymatic browning by natural extracts and genome-editing: a review on recent progress. *Molecules*. 2022;27(3). doi:10.3390/molecules27031101
12. Yildirim RM, Ergun Y, Basar M. Mitochondrial dysfunction, mitophagy and their correlation with perinatal complications: preeclampsia and low birth weight. *Biomedicines*. 2022;10(10). doi:10.3390/biomedicines10102539
13. Zhang H, Zheng Y, Liu X, et al. Autophagy attenuates placental apoptosis, oxidative stress and fetal growth restriction in pregnant ewes. *Environ Int*. 2023;173:107806. doi:10.1016/j.envint.2023.107806
14. Aye I, Aiken CE, Charnock-Jones DS, Smith GCS. Placental energy metabolism in health and disease-significance of development and implications for preeclampsia. *Am J Obstet Gynecol*. 2022;226(2S):S928–S944. doi:10.1016/j.ajog.2020.11.005
15. Wu Y, Li M, Ying H, et al. Mitochondrial quality control alterations and placenta-related disorders. *Front Physiol*. 2024;15:1344951. doi:10.3389/fphys.2024.1344951
16. Hu XQ, Zhang L. Hypoxia and mitochondrial dysfunction in pregnancy complications. *Antioxidants*. 2021;10(3). doi:10.3390/antiox10030405
17. Villalain C. Angiogenesis biomarkers and fetal growth restriction. *BJOG*. 2022;129(11):1878. doi:10.1111/1471-0528.17172
18. Pala S, Atilgan R, Ilhan N. High amniotic fluid fractalkine and MIP-1beta levels are associated with intrauterine growth restriction: a prospective cohort study. *Turk J Med Sci*. 2024;54(1):280–290. doi:10.55730/1300-0144.5789
19. Liu Z, Zhang K, Zhao Z, Qin Z, Tang H. Prognosis-related autophagy genes in female lung adenocarcinoma. *Medicine*. 2022;101(1):e28500. doi:10.1097/MD.0000000000028500
20. Meng C, Zhou JQ, Liao YS. Autophagy-related long non-coding RNA signature for ovarian cancer. *J Int Med Res*. 2020;48(11):300060520970761. doi:10.1177/0300060520970761
21. Zhu D, Zhang X, Fang Y, et al. Identification of a lactylation-related gene signature as the novel biomarkers for early diagnosis of acute myocardial infarction. *Int J Biol Macromol*. 2024;282(Pt 6):137431. doi:10.1016/j.ijbiomac.2024.137431
22. Jia Z, Zhang J, Li Z, Ai L. Identification of ferroptosis-related genes associated with diffuse large B-cell lymphoma via bioinformatics and machine learning approaches. *Int J Biol Macromol*. 2024;282(Pt 3):137117. doi:10.1016/j.ijbiomac.2024.137117
23. Nishizawa H, Ota S, Suzuki M, et al. Comparative gene expression profiling of placentas from patients with severe pre-eclampsia and unexplained fetal growth restriction. *Reprod Biol Endocrinol*. 2011;9:107. doi:10.1186/1477-7827-9-107
24. Bezemer RE, Schoots MH, Timmer A, et al. Altered levels of decidual immune cell subsets in fetal growth restriction, stillbirth, and placental pathology. *Front Immunol*. 2020;11:1898. doi:10.3389/fimmu.2020.01898
25. Zhu L, Li Q, Wang X, et al. THBS1 is a novel serum prognostic factors of acute myeloid leukemia. *Front Oncol*. 2019;9:1567. doi:10.3389/fonc.2019.01567
26. Chen C, Chen X, Yang S, et al. Association of THBS1 genetic variants and mRNA expression with the risks of ischemic stroke and long-term death after stroke. *Front Aging Neurosci*. 2022;14:1006473. doi:10.3389/fnagi.2022.1006473
27. Garcia-Conesa MT, Tribolo S, Guyot S, Tomas-Barberan FA, Kroon PA. Oligomeric procyanidins inhibit cell migration and modulate the expression of migration and proliferation associated genes in human umbilical vascular endothelial cells. *mol Nutr Food Res*. 2009;53(2):266–276. doi:10.1002/mnfr.200800134
28. Shang Y, Liu S, Liang C, et al. An integrated strategy of chemical fingerprint and network pharmacology for the discovery of efficacy-related Q-markers of pheretima. *Int J Anal Chem*. 2022;2022:8774913. doi:10.1155/2022/8774913
29. Ma J, Wu H, Yang X, Zheng L, Feng H, Yang L. Identification and validation of an angiogenesis-related signature associated with preeclampsia by bioinformatic analysis. *Medicine*. 2023;102(5):e32741. doi:10.1097/MD.0000000000032741
30. Isenberg JS, Roberts DD. THBS1 (thrombospondin-1). *Atlas Genet Cytogenet Oncol Haematol*. 2020;24(8):291–299. doi:10.4267/2042/70774
31. Yang N, Li M, Qin S, et al. Ehrlichia chaffeensis Etf-3 induces host RAB15 upregulation for bacterial intracellular growth. *Int J mol Sci*. 2024;25(5). doi:10.3390/ijms25052551
32. Zuk PA, Elferink LA. Rab15 differentially regulates early endocytic trafficking. *J Biol Chem*. 2000;275(35):26754–26764. doi:10.1074/jbc.M000344200
33. Zuk PA, Elferink LA. Rab15 mediates an early endocytic event in Chinese hamster ovary cells. *J Biol Chem*. 1999;274(32):22303–22312. doi:10.1074/jbc.274.32.22303
34. Strick DJ, Francescutti DM, Zhao Y, Elferink LA. Mammalian suppressor of Sec4 modulates the inhibitory effect of Rab15 during early endocytosis. *J Biol Chem*. 2002;277(36):32722–32729. doi:10.1074/jbc.M205101200
35. Matsuo T, Dat le T, Komatsu M, et al. Early growth response 4 is involved in cell proliferation of small cell lung cancer through transcriptional activation of its downstream genes. *PLoS One*. 2014;9(11):e113606. doi:10.1371/journal.pone.0113606
36. Nishimura N, Van Huyen Pham T, Hartomo TB, et al. Rab15 expression correlates with retinoic acid-induced differentiation of neuroblastoma cells. *Oncol Rep*. 2011;26(1):145–151. doi:10.3892/or.2011.1255
37. Wong P, Iwasaki A. RAB15 empowers dendritic cells to drive antiviral immunity. *Sci Immunol*. 2017;2(13). doi:10.1126/sciimmunol.aan6448
38. Nakamura H, Hori K, Tanaka-Okamoto M, et al. Decreased expression of LMO7 and its clinicopathological significance in human lung adenocarcinoma. *Exp Ther Med*. 2011;2(6):1053–1057. doi:10.3892/etm.2011.329
39. Guerin A, Roy NH, Kugler EM, et al. Cryptosporidium rhoptry effector protein ROP1 injected during invasion targets the host cytoskeletal modulator LMO7. *Cell Host Microbe*. 2021;29(9):1407–1420e5. doi:10.1016/j.chom.2021.07.002
40. Liu X, Yuan H, Zhou J, et al. LMO7 as an unrecognized factor promoting pancreatic cancer progression and metastasis. *Front Cell Dev Biol*. 2021;9:647387. doi:10.3389/fcell.2021.647387
41. Karlsson T, Kvarnbrink S, Holmlund C, et al. LMO7 and LIMCH1 interact with LRIG proteins in lung cancer, with prognostic implications for early-stage disease. *Lung Cancer*. 2018;125:174–184. doi:10.1016/j.lungcan.2018.09.017
42. Jiang ZR, Yang LH, Jin LZ, et al. Identification of novel cuproptosis-related lncRNA signatures to predict the prognosis and immune microenvironment of breast cancer patients. *Front Oncol*. 2022;12:988680. doi:10.3389/fonc.2022.988680
43. Duan S, Lou X, Chen S, et al. Macrophage LMO7 deficiency facilitates inflammatory injury via metabolic-epigenetic reprogramming. *Acta Pharm Sin B*. 2023;13(12):4785–4800. doi:10.1016/j.apsb.2023.09.012

44. Xu Y, Romero R, Miller D, et al. An M1-like macrophage polarization in decidual tissue during spontaneous preterm labor that is attenuated by rosiglitazone treatment. *J Immunol*. 2016;196(6):2476–2491. doi:10.4049/jimmunol.1502055
45. Wang WJ, Hao CF, Lin QD. Dysregulation of macrophage activation by decidual regulatory T cells in unexplained recurrent miscarriage patients. *J Reprod Immunol*. 2011;92(1–2):97–102. doi:10.1016/j.jri.2011.08.004
46. Guenther S, Vrekoussis T, Heublein S, et al. Decidual macrophages are significantly increased in spontaneous miscarriages and over-express FasL: a potential role for macrophages in trophoblast apoptosis. *Int J mol Sci*. 2012;13(7):9069–9080. doi:10.3390/ijms13079069